

Figure S1 related to Figure 1: Characterization of HTTex1 sensor proteins (A) Schematic representation of the applied GST-tagged HTTex1 fusion proteins with pathogenic and non-pathogenic polyQ tracts. P, proline-rich regions. (B) The recombinant GST-Ex1Q48-CyPet and -YPet fusion proteins were affinity purified using glutathione-coated sepharose beads. Purity was assessed by SDS-PAGE and subsequent Coomassie blue staining. (C) Investigation of PreScission protease (PSP)-mediated cleavage of GST-Ex1Q48-CyPet and -YPet fusion proteins. 3 μ M of GST fusion proteins were incubated in the presence or absence of PSP. Aliquots were taken at the indicated time points; cleavage was confirmed by SDS-PAGE and immunoblotting with a polyclonal anti-GFP antibody. (D) AFM analysis of co-aggregated sensor proteins Ex1Q48-CyPet/-YPet (3 μ M). Scale bar: 1 μ m; color gradient represents 0-20 nm height. (E) Preformed, fibrillar Ex1Q48 aggregates (seeds) shorten the lag phase of Ex1Q48-CyPet/-YPet polymerization; no

seeding effect was observed with the sensor proteins Ex1Q23-CyPet/-YPet. Seeds were produced by incubating GST-Ex1Q48 fusion protein with PSP for 24 h at 25 °C. Indicated seed concentrations are equivalent to monomer concentrations. Co-aggregation of the sensor proteins (1:1 mixture; 1.2 μ M) was monitored by quantification of FRET; the resulting aggregation kinetics were curve fitted by non-linear regression. FRET efficiency is plotted as means \pm SD of 3 technical replicates. (F) Ex1Q48-CyPet/-YPet (1:1 mixture; 3 μ M) sensor protein co-aggregation was accelerated by addition of preformed fibrillary Ex1Q48 seeds. Ex1Q23 protein was prepared under identical conditions (no fibrillar aggregates observed; data not shown). Co-aggregation of sensor proteins was not influenced by the addition of uncleaved GST-Ex1Q48 or GST-Ex1Q23 fusion proteins, respectively. Co-aggregation of the fluorescence sensor proteins was monitored by quantification of FRET; the resulting aggregation kinetics were curve fitted by non-linear regression. Indicated seed concentrations are equivalent to monomer concentrations. Data is shown as means \pm SD of 3 technical replicates.

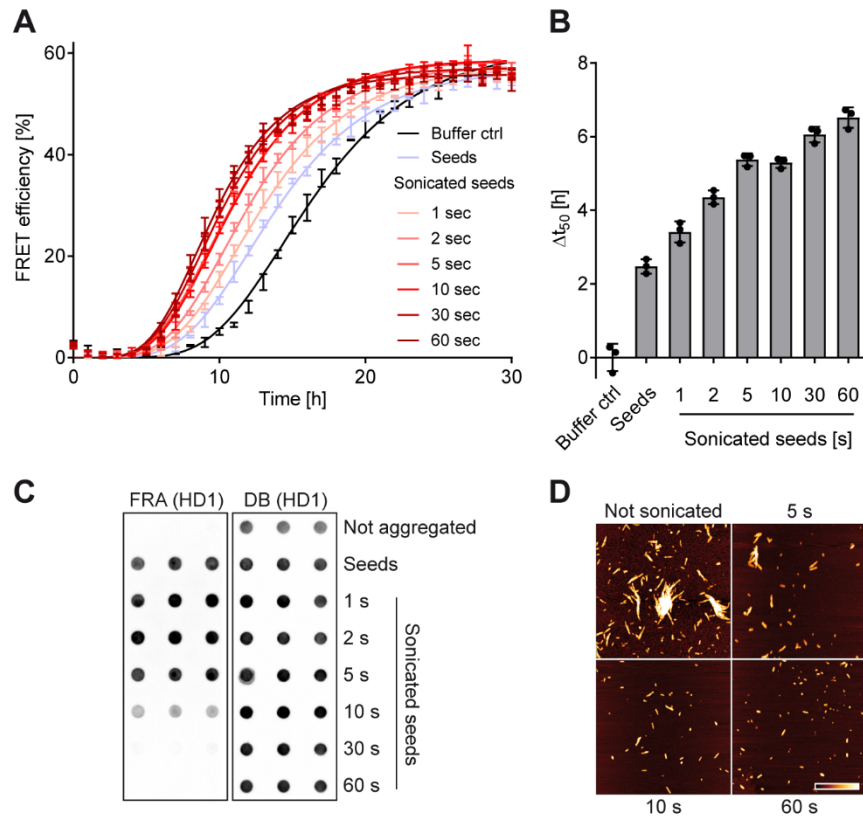


Figure S2 related to Figure 2. Both small and large fibrillar Ex1Q48 aggregates exhibit seeding activity in FRASE assays (A) Sonication of preformed, fibrillar Ex1Q48 aggregates reveals protein fractions with high HSA in FRASE assays. Fibrillar Ex1Q48 aggregates were produced by incubating GST-Ex1Q48 fusion protein (2 μ M) for 24 h at 25 $^{\circ}$ C. 1 nM preformed Ex1Q48 aggregates (seeds) were added to Ex1Q48-CyPet/-YPet (1:1 mixture; 1.2 μ M) co-aggregation reactions. The added seed concentration is equivalent to the monomer concentration. Data is shown as means \pm SD of 3 technical replicates. (B) Quantification of HSA. Calculated Δt_{50} values from Ex1Q48-CyPet/-YPet aggregation profiles in **A**. Δt_{50} is displayed as individual values (\bullet) and mean \pm SD of technical triplicates. (C) Analysis of sonicated and non-sonicated Ex1Q48 seeds by denaturing filter retardation (FRA, left panel) and dot blot (DB, right panel) assays. Fragmentation of large fibrillar Ex1Q48 aggregates by sonication prevents their detection by FRAs. (D) Preformed Ex1Q48 fibrils were sonicated for the indicated times and visualized by AFM. Sonication reduces the size of preformed Ex1Q48 fibrils. Scale bar: 1 μ m; color gradient represents 0-20 nm height.

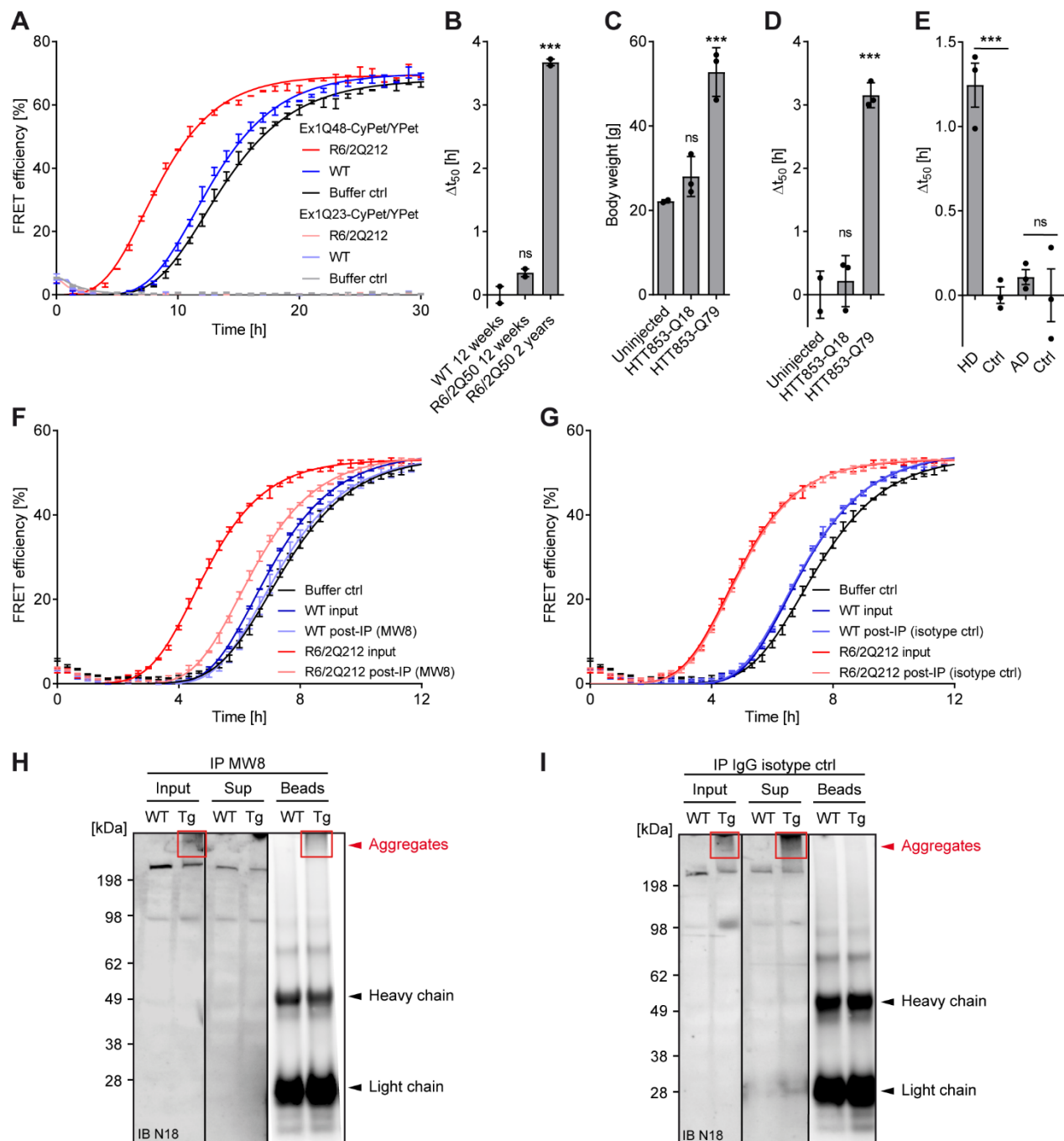


Figure S3 related to Figure 3. Detection of mHTT seeding activity in brain extracts of various HD mouse models

(A) Brain homogenates (7.5 μ g) prepared from R6/2Q212 and WT mice were added to Ex1Q48-CyPet/-YPet or Ex1Q23-CyPet/-YPet sensor proteins. Brain homogenates prepared from R6/2Q212 mice accelerated Ex1Q48-CyPet/-YPet polymerization but do not induce co-aggregation of Ex1Q23-CyPet/-YPet sensor proteins. Co-aggregation of sensor proteins (1:1 mixture; 1.2 μ M) was monitored by quantification of FRET and displayed as mean \pm SD of technical triplicates; the resulting aggregation kinetics were curve fitted by non-linear regression. (B) Quantification of HSA in brain extracts prepared from R6/2Q51 transgenic mice and controls using FRASE assays (1.2 μ M Ex1Q48-CyPet/-YPet). HSA measured for each mouse is displayed as dots (\bullet). Bars are mean \pm SEM. Statistical significance was assessed by One-Way ANOVA followed by Dunnett's multiple comparisons test ($n = 2$). (C) Analysis of body weight of FVB/N mice expressing the proteins HTT853Q18 or HTT853Q79 for 8 weeks. Body weight of individual mice is

displayed as dots (●). Bars are mean \pm SEM. Statistical significance was assessed by One-Way ANOVA followed by Dunnett's multiple comparisons test ($n = 3$). (D) Quantification of HSA in hypothalamic brain homogenates of FVB/N mice expressing the proteins HTT853Q18 or HTT853Q79. The total concentration of sensor proteins was 3 μ M. Data are mean \pm SEM ($n = 3$). Individual measurements are displayed as dots (●). Statistical significance was assessed by One-Way ANOVA followed by Dunnett's multiple comparisons test. (E) Brain homogenates prepared from tissues of HD (caudate nucleus) and AD (temporal cortex) patients were analyzed by FRASE assays and compared to corresponding brain tissue of control individuals. HSA values are plotted individually as dots (●) and as mean \pm SEM ($n = 3$); caudate tissue from HD patients (Grade 4, CAG repeat length: 52.3 ± 1.2 , Age 42.3 ± 2.1), caudate tissue from controls (Age 60.3 ± 1.2), cortical tissue from AD patients (Braak 6, Age 73.3 ± 4.6), cortical tissue from controls (Braak 0, Age 66.3 ± 7). Statistical significance was assessed by unpaired t test. (F) Immunodepletion of mHTT_{ex1} aggregates from R6/2Q212 mouse brain homogenates decreases their seeding activity in FRASE assays. Brain homogenates prepared from transgenic mice and littermate controls (12 weeks) were incubated with MW8 antibody-coated protein G beads; supernatant (post-IP) and input samples were applied to FRASE analysis using 3 μ M of sensor proteins. FRET efficiency is plotted as mean \pm SD of technical triplicates. (G) Same procedure as in **F** but with an IgG isotype control antibody. (H and I) Immunoblots of samples analyzed in **F** and **G**. mHTT_{ex1} aggregates appear as a smear at the upper edge of the blot (red rectangles). Input, brain extract before immunodepletion; Sup, supernatant after immunodepletion; Beads, antibody-coated protein G beads after immunodepletion. mHTT_{ex1} aggregates are depleted from mouse brain homogenates with the anti-HTT antibody MW8 but not with an IgG isotype control antibody.

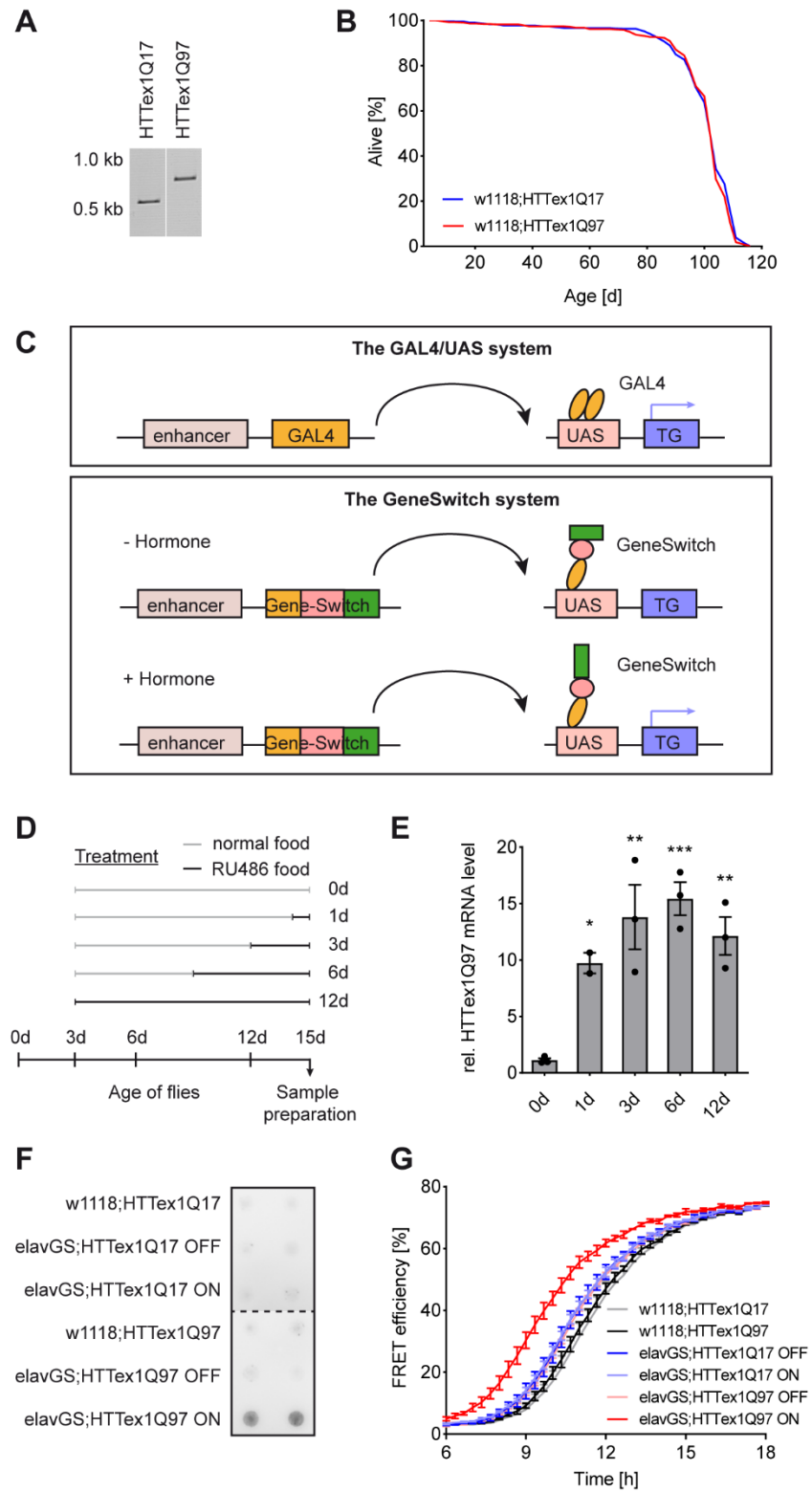


Figure S4 related to Figure 5. Temporal regulation of HTTex1Q97 transgene expression in a newly generated *Drosophila* model of HD (A) Confirmation of fly strain identity by PCR-based genotyping. Expected sizes of PCR products: 526 bp (HTTex1Q17) and 766 bp (HTTex1Q97). (B) Life span analysis of w1118;HTTex1Q97 and

w¹¹¹⁸;HTTex1Q17 flies ($n^{w^{1118};HTTex1Q17} = 92, 176, 98$; $n^{w^{1118};HTTex1Q17} = 88, 148, 93$). Life span is plotted as the percentage of surviving flies of 3 biological replicates. (C) Schematic illustration of the GAL4/UAS and the Gene-Switch expression system. The yeast transcription activator GAL4 binds to the UAS sequence and activates the transcription of the transgene (TG) cloned downstream of the UAS. The Gene-Switch system is based on a GAL4-progesterone receptor fusion protein which is not transcriptionally active until induced by steroids (RU486). This allows regulation of transgene expression. (D) Schematic illustration of the RU486 treatment used to induce HTTex1Q97 expression. Grey lines, no treatment; black lines, RU486 treatment. (E) qPCR analysis of induction of HTTex1Q97 transcription upon treatment with the inducer hormone RU486. The rp49 gene was used as reference gene. Results are depicted individually (●) and as mean \pm SEM of 3 biological replicates; statistical significance was assessed by One-way ANOVA Dunnett's post-hoc test. (F) Analysis of mHTTex1 aggregate load in fly heads by FRAs immunodetected with the MW8 antibody. Two biological replicates are depicted per condition. (G) FRASE analysis of head lysates from flies analyzed in **F**. Values are plotted as means \pm SEM of 3 biological replicates each performed in triplicates.

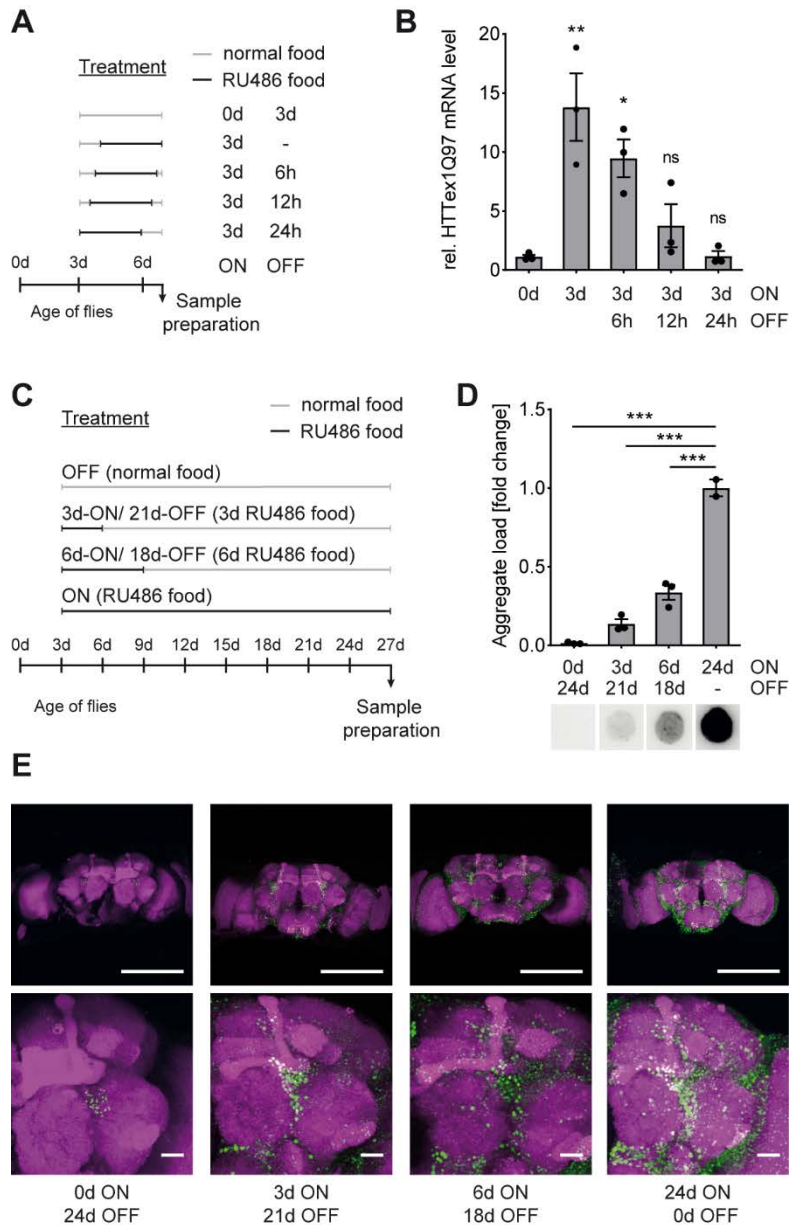


Figure S5 related to Figure 5. Detection of mHTTex1 aggregates in *Drosophila* HD models (A) Illustration of hormone treatment utilized to assess the dynamics of HTTex1Q97 transcriptional repression upon hormone removal. Grey lines indicate time periods without RU486 treatment; black lines indicate time periods of exposure to RU486. (B) Relative mRNA levels assessed by qPCR show transcriptional repression of HTTex1Q97 upon removal of RU486. Values are depicted as mean \pm SEM of 3 biological replicates; individual measurements (\bullet); significance assessment with One-way ANOVA Dunnett's post-hoc test. (C) Treatment scheme for the preparation of *Drosophila* samples for FRA and FRASE analyses. (D) Analysis of mHTTex1 aggregate load in fly head lysates by FRAs (75 μ g protein) using the MAB5492 antibody. Data is displayed as mean \pm SEM of 3 biological replicates; individual measurements (\bullet); statistical significance was assessed by One-way ANOVA Dunnett's post-hoc test. (E) Representative confocal images of elavGS;HTTex1Q97 whole fly brains (hormone treatment as in C. The RBP staining is shown in magenta and the MAB5492 staining in green (Scale bars: 200 μ m). Magnifications are shown below (Scale bars: 20 μ m).

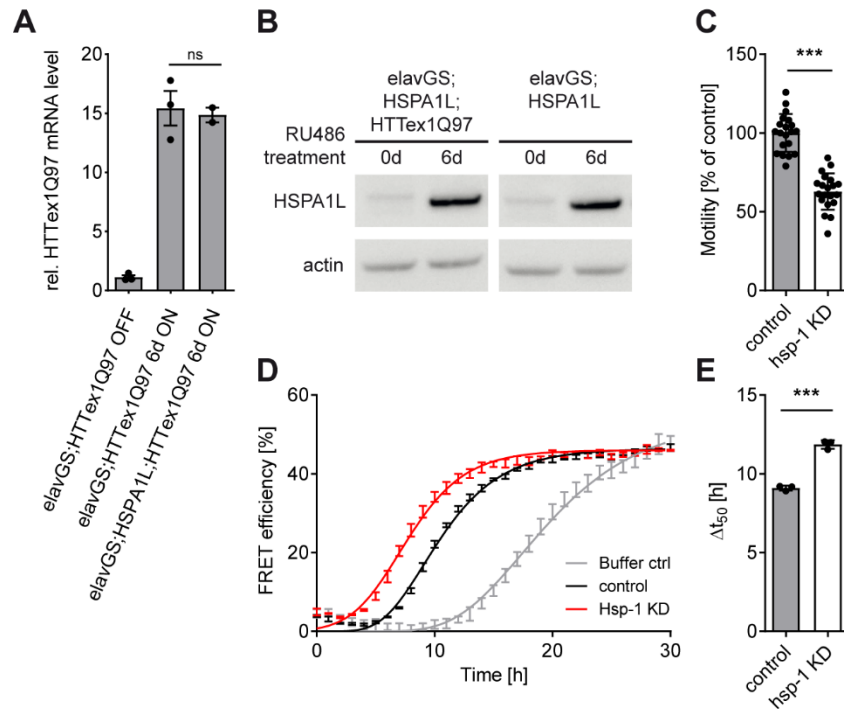


Figure S6 related to Figure 6. Effects of chaperone levels on HSA in transgenic flies and worms (A) Relative mRNA levels assessed by qPCR show similar expression of HTTEx1Q97 in elavGS;HTTEx1Q97 and elavGS;HSPA1L;HTTEx1Q97 flies. Bars are mean \pm SEM of three biological replicates and individual measurements are displayed as dots (\bullet); significance assessment with unpaired t-test. (B) Comparison of Hsp70 protein levels in elavGS;HSPA1L;HTTEx1Q97 and elavGS;HSPA1L flies untreated and treatment with RU486. Protein extracts prepared from fly heads were analyzed by SDS-PAGE and immunoblotting (20 μ g of total protein). (C) Motility phenotype (% motility) of RNAi-treated and untreated Q35-YFP expressing transgenic worms at day 5. In all cases, data were normalized to age-matched control worms. Data are mean \pm SEM (n = 20). Significance assessment with unpaired t test. (D) FRASE analysis of Q35-YFP seeding activity in RNAi-treated and untreated worms after 5 days. FRET efficiency is displayed as mean \pm SD. (E) Quantification of results shown in **D**. HSA values are plotted individually as dots (\bullet) and as mean \pm SD.